Desalination and Water Treatment
www.deswater.com
doi: 10.1080/19443994.2014.899927

54 (2015) 2581–2591
May

Taylor & Francis
Taylor & Francis Group

Preparation of Pd-doped nano-TiO_2 in microemulsion and their application in photodegradation of C.I. Acid Yellow 23

R. Najjar[a,*], M. Shokri[b], S. Farsadi[b]

[a] *Faculty of Chemistry, Polymer Research Laboratory, University of Tabriz, Tabriz, Iran, Tel. +98 411 3393101; Fax: +98 411 3340191; email: najjar@tabrizu.ac.ir*
[b] *Department of Applied Chemistry, Islamic Azad University, Tabriz Branch, Tabriz, Iran*

Received 5 June 2013; Accepted 21 February 2014

ABSTRACT

In this paper, the application of palladium-doped TiO_2 nanoparticles (Pd/TiO_2) in photocatalytic degradation of the C.I. Acid Yellow 23 (AY23) dye as a water pollutant under UV light illumination and their synthesis via microemulsion method is reported. The prepared catalysts were characterized using transmission electron microscopy, scanning electron microscopy, XRD, and energy-dispersive X-ray techniques. The effect of parameters such as Pd loading, photocatalyst dosage, initial dye concentration, and calcinations temperature on the photocatalytic activity of the catalysts was investigated. The optimum conditions leading to the highest photonic efficiency were found to be using of 0.75 wt% of Pd loading on TiO_2, photocatalyst dosage of 600 mg L^{-1}, and calcination temperature of 300°C for initial dye concentration of 0.05 mM. A complete decolorization of 0.05 mM AY23 dye solution under UV irradiation at optimum conditions on Pd/TiO_2 was observed in 30 min.

Keywords: Acid Yellow 23; Heterogeneous photocatalysis; Pd-doped TiO_2; Microemulsion; UV/TiO_2

---

1. Introduction

Titanium dioxide (TiO_2) is one of the oxide semiconductors with excellent capabilities that has been considered as a good candidate for widespread photocatalytic applications. The biological and chemical inertness, low cost, availability, strong oxidizing power, non-toxicity, and long-term stability against photo and chemical corrosion are among its capabilities that make it useful in many applications [1].

However, the TiO_2 photocatalyst has two limitations for practical applications: (a) the wavelength range of activity of TiO_2 lies lower than 388 nm, which is because of its wide band gap ($E_g = 3.2$ eV), and this limits the use of sunlight as an excitation energy source, (b) another problem is that the high recombination rate of photo-generated electron-hole pairs in TiO_2 results in the low photo quantum efficiency [2]. Hence, many efforts have been devoted to overcome or reduce the effects of these limitations.

In order to increase the activity of TiO_2 and extend its response range to the wavelengths in visible region, TiO_2 nanoparticles have been modified by different methods. These methods include doping of metallic or non-metallic ions into the TiO_2 lattice, dye photosensitization on the TiO_2 surface, addition of inert support, semiconductor coupling, and deposition of noble metals [1,3]. It has been found that, the nanosized noble

---

*Corresponding author.

metal particles dispersed on the TiO_2 support act as electron sinks, resulting in a decrease in the electron-hole recombination as well as the efficient charge separation during photocatalysis [4]. The noble metal can effectively suppress undesired redox reactions that consume photogenerated radicals [5] and also prevent the deactivation of the photocatalyst at high temperatures [6]. Meanwhile, negative effect of the Pd doping on the activity of TiO_2 nanoparticles in photodegradation of 1,2-dichloroethane has been reported, which was attributed to the possible effect of Pd ions in increasing the adsorption of byproducts on the surface of TiO_2, and consequently reducing the number of available active sites for the photocatalytic reaction [7]. The presence of PdO on the Pd-doped TiO_2 photocatalysts has been confirmed as the active form of Pd on the catalyts [8,9].

Acid Yellow 23 (AY23) or Tartrazine (Fig. 1) is an anionic azo dye present in thousands of textiles (as a dye for wool and silk), foodstuff, and pharmaceutical wastewaters [10,11]. The decolorization of AY23 or other typical azo dyes has been reported by several methods, such as biological [12], adsorption [13], Fenton and photo-Fenton [14], UV/H_2O_2 [15], UV-irradiated ZnO/SnO_2 photocatalysts [16], electrocoagulation [10], polystyrene anion exchangers [17], photocatalytic degradation by dispersed or immobilized ZnO [18] and TiO_2 [19,20] on glass plates and photodegradation by metal-doped TiO_2 [21–23].

Nevertheless, several reports have been published in the literature concerning the photocatalytic degradation of pollutants on Pd-loaded TiO_2 catalysts prepared by different methods [24–27]. To the best of our knowledge, there is no systematic study dealing with the photocatalytic degradation of dyes with the Pd-loaded TiO_2 prepared via microemulsions.

Microemulsions or micelles (including reverse micelles) represent an approach based on the formation of micro/nano-sized reaction vessels for the preparation of nanoparticles. Hence, they have received considerable attention in recent years by development of nanosciences [28–30]. The various aspects of microemulsions, including their properties and applications have been detailed elsewhere [31].

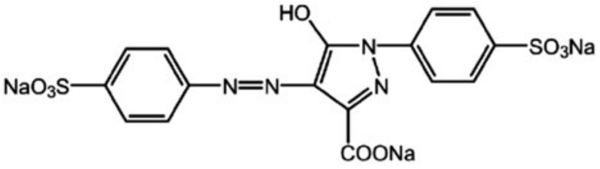

Fig. 1. The molecular structure of Acid Yellow 23 dye.

This is the first report on the preparation of Pd-doped TiO_2 by microemulsion method, and also the first study dealing with the removal of AY23 using metal-doped TiO_2 photocatalyst. In this work, Pd-doped TiO_2 nanoparticles were prepared via two microemulsions method and their structure were confirmed with different techniques. Then, the photocatalytic degradation of AY23, as a model pollutant, on the prepared Pd-loaded TiO_2 nanoparticles (Pd/TiO_2), was studied. We have systematically optimized the parameters, such as photocatalyst dosage, doping content, and effect of calcination temperature on the photocatalytic oxidation of AY23 as a representative mono azo dye, under the illumination of UV light. The extent of photodegradation and mineralization was measured by UV–Vis spectrometer and total organic carbon (TOC) analyzer, respectively.

2. Experimental

2.1. Materials

Sodium bis(2-ethylhexyl) sulfosuccinate (AOT, 96%) was obtained from Acros Organics. Palladium (II) chloride ($PdCl_2$, 59% Pd), sodium borohydride (98%, Merck), and *n*-heptane (>99%, HPLC grade, Scharlau) were used as received without any further purification. TiO_2-P25 Degussa ca. 80% anatase, 20% rutile, BET surface area, ca. 50 m^2/g; primary size ~21 nm were used as a supporting material. AY23 was purchased from Acros Organics (USA). The AY23 is a monoazo anionic dye (heterocyclic azo dye) with C.I. number 19,140 and λ_{max} 428 nm.

2.2. Preparation of Pd/TiO_2 photocatalyst

The Pd/TiO_2 photocatalysts were prepared using two microemulsion method, namely reducing agent and metal precursor containing microemulsions (*n*-heptane/AOT/water/$PdCl_2$ or $NaBH_4$). The metal precursor and reducing agent containing microemulsions were prepared by mixing of the desired amounts of the proper chemicals to obtain the molar ratios of $[H_2O]/[AOT] = 10$, [*n*-heptane/water] = 250 and aqueous phase concentrations of $[NaBH_4] = 0.3$ M and $[Pd^{2+}] = 0.1$ M. In addition, proper amount of theTiO_2-P25 was added to the vigorously stirred metal precursor containing microemulsion to obtain the Pd loadings of 0.125, 0.25, 0.5, 0.75, and 1 wt% relative to TiO_2. For preparation of the Pd/TiO_2 nanoparticles, the same volume of reducing agent containing microemulsion was added dropwise during 60 s to the metal precursor microemulsion containing adequate amount of TiO_2, and the mixture was kept under vigorous stirring by magnetic stirrer for 45 min. All reactions were performed at the room temperature without the removal of air. Acetone was used to break the microemulsion and precipitate out the nanoparticles. Finally, the precipitate was washed with ethanol to remove the remaining AOT. The nanoparticles were obtained by centrifuging the washed precipitate at 5,000 rpm for 15 min, dried at 100˚C for 12 h, and finally calcined at desired temperature (300, 450, 600, or 750˚C) for 3 h.

2.3. Characterization and measurements

Morphology of Pd/TiO_2 nanoparticles was characterized by transmission electron microscopy (TEM, Zeiss EM900-80 keV). A Shimadzu UV–Vis spectrophotometer (model UV-1700) was used to record the absorbances as the reaction proceeded. The crystalline phase of nanoparticles was analyzed by X-ray diffraction measurements using a Siemens XRD-D5000 ($\lambda = 0.154$ nm). Scanning electron microscopy (SEM) analysis was performed on Au-coated samples using a Philips apparatus model XL30, equipped with a probe for the energy-dispersive X-ray (EDX) analysis. The extent of Pd loading was analyzed using a Varian atomic absorption spectrophotometer (AAS, model AA240).

An ultrasonic bath from Elma (model T 460/H, Germany) was employed for sonication of the samples. A UV lamp (15 W, UV-C, $\lambda_{max} = 254$ nm, manufactured by Philips, the Netherlands) was used as the excitation source. The concentration of AY23 was measured by using a UV–Vis spectrophotometer (Ultrospec 2000, England). The concentration of total dissolved organic carbon (TOC) in the solution was analyzed using a TOC analyzer (Shimadzu, TOC-V_{CSH}) equipped with a non-dispersive infrared (NDIR) detector. The TOC was calculated as the difference between total carbon and inorganic carbon.

For the photocatalytic degradation studies, a desired amount of photocatalyst (pure or Pd doped TiO_2 nanoparticles) was added to the doubly distillated water and sonicated for 15 min to obtain a uniform suspension. Then, a proper amount of the AY23 stock solution was added to the photocatalyst suspension to achieve desired concentration of dye. The samples were then agitated for 30 min in the darkness to ensure the establishment of adsorption–desorption equilibrium of the dye on the photocatalyst surface. Afterwards, 100 ml of the above suspension was transferred into a borosilicate Petri dish of diameter 12 cm and height 1.5 cm taken as a photoreactor, and while vigorous stirring, the reaction mixture was UV irradiated from top of the solution with a 15 W UV lamp. In the whole experiment, the distance of the lamp from the solution was adjusted in such a way to obtain a light intensity of 35 W/m^2 on the surface of solution (measured by Lux-UV-IR meter, Leybold Co.).

At certain reaction intervals, 5 ml of sample was withdrawn, centrifuged for 15 min at 5,000 rpm and after the removal of solids, the concentration of AY23 was determined by means of a UV–Vis spectrophotometer at 428 nm using a calibration curve. All photodegradation experiments were carried out at room temperature on 0.05 mM solutions of AY23 with pH of about 6.5, which is the natural pH of the reaction medium.

3. Results and discussion

3.1. The characterization of Pd/TiO_2 nanoparticles

The prepared Pd/TiO_2 nanoparticles were characterized using TEM, SEM, XRD, and EDX techniques. The size of Pd nanoparticles was measured from the TEM micrographs (Fig. 2), to be around 5–15 nm, and almost uniformly distributed on the TiO_2 particles.

As can be seen from SEM images in Fig. 3(a) and (b), the spherical shape of TiO_2 was unchanged by Pd loading using microemulsion method. The EDX analysis (Fig. 3(c)) also confirmed the loading of Pd on TiO_2.

The XRD patterns of TiO_2 and Pd/TiO_2 nanoparticles (0.75 wt% Pd) are evaluated in the range of 2θ values of 20˚–70˚. All photocatalyst samples show the dominant anatase peaks at $2\theta = 25.2˚$, 38˚, 48.2˚, 55˚, and 62.5˚ and the small fraction of rutile phase with peaks at $2\theta = 27.5˚$, 36˚, 54˚, and 69˚. The XRD patterns of Pd/TiO_2 samples almost coincide with that of pure TiO_2 showing no diffraction peaks (at $2\theta = 40.1˚$, 46.9˚) due to Pd doping, thus suggesting that the microemulsion method yields uniformly dispersed palladium nanoparticles on the TiO_2 [25]. The Pd content of the synthesized photocatalysts was determined by AAS analysis of the remaining Pd in the filtrate after separation of the photocatalyst. The measured Pd contents by AAS are given in Table 1. The results indicate that the actual Pd content of the photocatalysts is almost equal to the planned values to be obtained by the microemulsions.

3.2. Photocatalytic activity studies

The effects of different parameters on the photocatalytic activity of the prepared samples have been studied. The results indicated that the doping of Pd

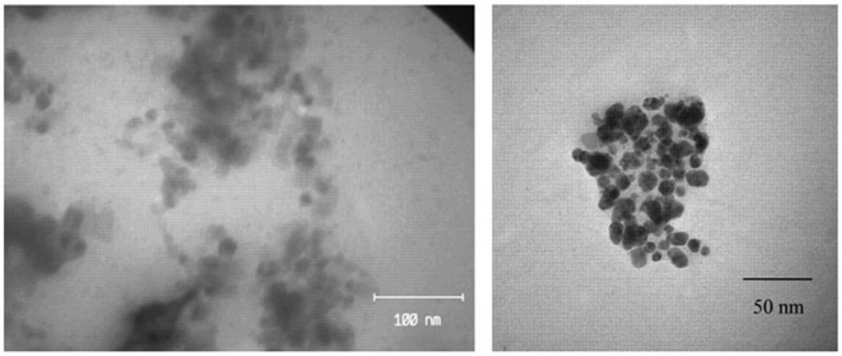

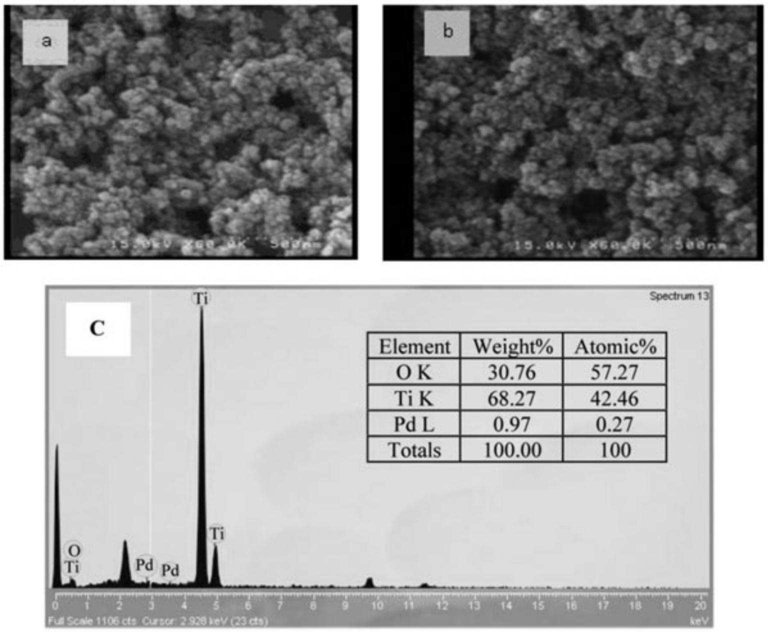

Element	Weight%	Atomic%
O K	30.76	57.27
Ti K	68.27	42.46
Pd L	0.97	0.27
Totals	100.00	100

Fig. 3. (a) SEM micrograph of TiO_2, (b, c) SEM micrograph and EDX spectra of 0.75 wt% Pd/TiO_2 nanoparticles prepared by microemulsion method.

Table 1
Pd content of Pd /TiO_2 photocatalyst measured by AAS

Catalyst	Pd content (wt%)
TiO_2–P25	0
0.25 wt% Pd/TiO_2	0.248
0.5 wt% Pd/TiO_2	0.495
0.75 wt% Pd/TiO_2	0.742
1 wt% Pd/TiO_2	0.99
1.5 wt% Pd/TiO_2	1.48

on the commercial TiO_2 nanoparticles has improved their photocatalytic activity. The results will be detailed in the next sections. The mechanism of the photodegradation process on the TiO_2 photocatalyst has been already reviewed elsewhere [32]. It has been confirmed that the •OH radicals produced on the surface of TiO_2 are responsible for the heterogeneous photodegradation of organic molecules, such as dyes, on the TiO_2. The evaluation of the degradation products and their toxicological properties is very important. The investigation of the similar dyes has revealed that byproducts of degradation reaction are compounds, such as sulfanilic acids, benzene sulfonates and 4-hydroxybenzene sulfonic acid [32,33] and the reaction routes for their formation were explained. These intermediates are mainly more friendly compounds to the environment than the degraded dyes. Therefore, even in case of decolorization or partial degradation, i.e. incomplete mineralization, the process significantly reduces the environmental effects of the mentioned pollutants. According to the literature, absorbed oxygen on the photocatalyst plays an important role in scavenging of photogenerated electrons, and also prevents the recombination of the photogenerated electrons and the oxidized dye radicals [33]. Hence, in this study all the samples were stirred in the darkness for 30 min to ensure that almost the same level of oxygen was absorbed on the surface of photocatalyst.

3.2.1. UV–Visible spectrophotometry

The typical time-dependent UV–Vis spectrum of AY23 solution during photocatalytic degradation of 0.05 mM solutions of dye using 200 mg L^{-1} of a pure TiO_2 or Pd/TiO_2 (0.75 wt%) photocatalysts calcined at 300℃ is shown in Fig. 4(a) and (b), respectively. The UV–Vis spectrum of the reaction mixture shows a decreasing trend in the intensity with reaction time for all of the observed peaks in the entire range of UV and visible region, and finally, they disappear. These observations indicate the gradual degradation of the dye.

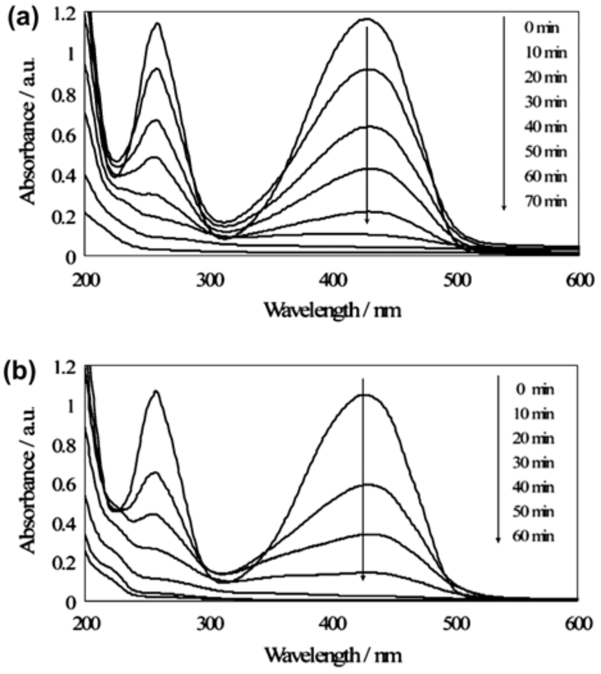

Fig. 4. Time-dependent UV–Vis spectrum of 0.05 mM solution of AY23 irradiated with UV light in the presence of 200 mg L^{-1} of: (a) pure TiO_2 (b) 0.75 wt% Pd/TiO_2 photocatalysts calcined at 300℃.

3.2.2. The effect of Pd loading

The degradation efficiency (%) could be calculated by:

$$D(\%) = 100 \times \frac{(C_o - C_t)}{C_o} \qquad (1)$$

where D is the degradation efficiency (%), C_o is the initial concentration, and C_t is the concentration of AY23 at any time after the start of irradiation with UV light.

For investigation of the effect of Pd loading on the photocatalytic degradation efficiency of the photocatalysts, the variations in concentration of the AY23 with reaction time were measured using the absorption peak intensity at wavelength of 428 nm. The ratio of AY23 concentration after any reaction time to its initial concentration (C/C_o) for the photodegradation reactions carried out using 200 mg L^{-1} photocatalysts with different Pd loadings was calculated and C/C_o was plotted vs. reaction time in Fig. 5. As can be seen in Fig. 5, the photocatalytic activity of the photocatalyst increases with increase in the Pd loadings up to certain level (optimum metal loading) and then decreases. The detrimental effect of increasing Pd loading on the photocatalytic activity of TiO_2 was explained by several ways in the literature, such as:

(1) The excess loading of metal particles may cover active sites on the TiO_2 surface, thereby, reducing photodegradation efficiency [25].
(2) Negatively charged Pd sites attract holes and, subsequently, recombine them with electrons. With increasing the Pd loading, and conse-

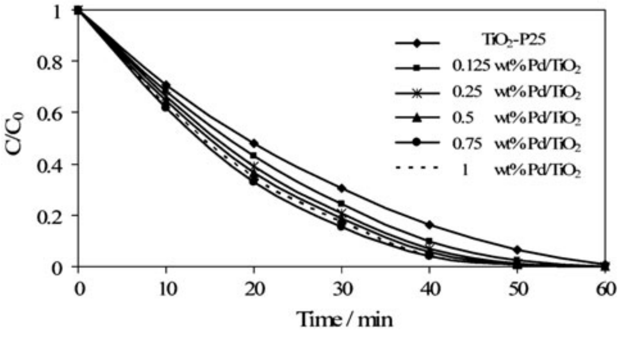

Fig. 5. AY23 concentration ratio as a function of exposure time under different Pd loadings (initial AY23 concentration, 0.05 mM; initial solution pH, 6.5; [photocatalyst] = 200 mg L^{-1}).

quently Pd sites, the metal deposits become recombination centers for holes and electrons [34].

3.3. The effect of photocatalyst dosage

The effect of photocatalyst dosage was determined by experiments carried out at constant AY23 concentration of 0.05 mM, while the photocatalyst dosage was varied from 100 to 800 mg L^{-1}. In Fig. 6, the (C/C_o) values were plotted vs. reaction time for the AY23 photodegradations carried out using 0.75 wt% Pd/TiO_2 photocatalyst (optimum Pd loading) with the different photocatalyst dosages. The results showed that the AY23 photodegradation rate changes with the dosage of Pd/TiO_2. The degradation efficiencies of AY23 achieved using 0.75 wt% Pd/TiO_2 photocatalyst (optimum Pd loading) with the different photocatalyst dosages vs. time are given in Table 2. It can be seen that in the experiment with 600 mg L^{-1} of photocatalyst with 0.75 wt% Pd loading, after 30 min of UV irradiation, the degradation efficiency (D(%)) has reached to about 98.6%.

When the initial dye concentration (C_o) is in the millimolar range (dilute solution), the rate equation simply can be written as an apparent first-order rate equation, Eq. (2):

$$-\ln[C/C_o] = k_{\text{app}} \cdot t \tag{2}$$

A plot of $-\ln[C/C_o]$ vs. time represents a straight line, the slope of the best line fitted to the data points equals to the apparent first-order rate constant k_{app} [32].

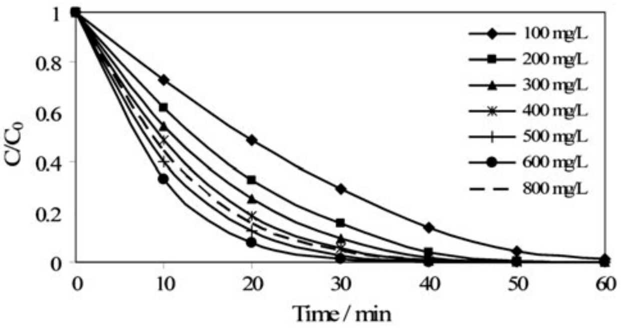

Fig. 6. AY23 concentration ratio as a function of exposure time under different dosages of 0.75 wt% Pd/TiO_2 photocatalyst calcined at 300˚C (initial AY23 concentration = 0.05 mM).

Linear regression analysis of the plots has presented a good fit to the data points with R^2 values of higher than 0.987, which confirms the first-order kinetic of the reaction. The degradation efficiencies (D(%)) as well as k_{app} values calculated for photocatalysts with different dosages of 0.75 wt% Pd/TiO_2 photocatalyst after 30 min of photodegradation reaction (highlighted raw in Table 2) are given in Table 3. As can be seen in Table 3, at 0–30 min irradiation time, the highest calculated k_{app} (0.1419 s^{-1}) and degradation efficiency (98.6%) values imply that 600 mg L^{-1} of 0.75 wt% Pd loading on the TiO_2 is the optimum value to obtain the highest photocatalytic activity.

The increase of the photocatalyst dosage results in an increase of the rate of generation of active species reacting with the dye molecules, consequently, increasing the photodegradation reaction rate. However, increasing of the Pd/TiO_2 dosage to higher than 600 mg L^{-1} limits the intensity of light penetrating into the reaction medium [35], and also increases the unfavorable light scattering [36], and, hence, inversely affects the photocatalytic reaction.

3.3.1. The effect of calcination temperature

In order to study the influence of the calcination temperature on the photocatalytic activity of photocatalyst, the samples of 0.75 wt% Pd/TiO_2 catalyst (optimum Pd content) were calcined at 300, 450, 600, and 750˚C for 3 h. Then, 600 mg L^{-1} of each of these samples was employed in a photodegradation experiments, while the other experimental conditions were kept the same (initial AY23 concentration = 0.05 mM). According to the results, depicted in Fig. 7, the photocatalytic activity of Pd/TiO_2 catalysts was decreased with increasing of the calcination temperature, and the highest photodegradation activity was achieved for the catalyst calcined at 300˚C. Already, it has been reported that the increase of the calcination temperature for the metal doped TiO_2 photocatalysts from 300 to 500˚C promote the formation of the more anatase phase, which has higher photocatalytic activity [37]. Meanwhile, by increasing of the calcination temperature to higher than 600˚C, anatase phase begins to transform to rutile phase, which exhibited lower photocatalytic activity. On the other hand, the conglomeration of catalyst particles was reported with increasing of the calcination temperature [38], causing reduction in specific surface areas of the samples, and consequently the catalyst calcined at higher temperature has a lower photocatalytic activity. Hence, increasing of the calcination temperature has diverse effects on the photocatalytic activity of the catalyst. As

Table 2
The photodegradation efficiencies of AY23 vs. time using different dosages of 0.75 wt% Pd/TiO_2 photocatalyst, calcined at 300℃ (initial AY23 concentration = 0.05 mM)

	Degradation efficiency (*D*%)						
Time (min)	100 mg L^{-1}	200 mg L^{-1}	300 mg L^{-1}	400 mg L^{-1}	500 mg L^{-1}	600 mg L^{-1}	800 mg L^{-1}
10	27.13	38.29	45.81	51.42	59.73	66.99	55.56
20	51.24	67.24	74.63	81.57	87.49	92.09	84.32
30	70.88	84.36	90.45	94.48	97.26	98.56	95.31
40	86.19	96.11	98.24	99.40	99.61	100	99.19
50	95.52	99.36	99.74	100	100	100	99.84
60	98.83	100	100	100	100	100	100

Table 3
The degradation efficiencies and k_{app} and R^2 values obtained for the photodegradation of AY23 after 30 min reaction for different dosages of 0.75 wt% Pd/TiO_2 photocatalyst calcined at 300℃ (initial AY23 concentration = 0.05 mM)

Dosage of photocatalyst	100 mg L^{-1}	200 mg L^{-1}	300 mg L^{-1}	400 mg L^{-1}	500 mg L^{-1}	600 mg L^{-1}	800 mg L^{-1}
D (%)	70.88	84.36	90.45	94.48	97.26	98.56	95.31
k_{app} (s^{-1})	0.041	0.062	0.078	0.096	0.120	0.142	0.102
R^2	0.988	0.991	0.989	0.987	0.987	0.990	0.992

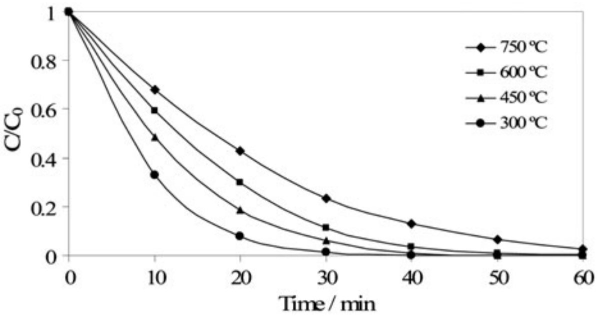

Fig. 7. AY23 concentration ratio as a function of exposure time using 600 mg L^{-1} of 0.75 wt% Pd/TiO_2 photocatalyst calcined at different temperatures (initial AY23 concentration = 0.05 mM).

the catalyst calcined at 300℃ has presented the highest photocatalytic activity, implies that the decreasing effect of the conglomeration of catalyst particles is much more pronounced compared to the increasing effect of the formation of the anatase phase. The mentioned reports mainly dealt with the effect of calcination temperature, either on the support particles, such as carbon-supported Au–Pd catalysts [39], Pd on the porous Nb_2O_5 and Ta_2O_5 supports [40] or on the agglomerates of the precursor salts impregnated on the supports, i.e. before reduction of the salts to metallic nanoparticles, Pd/SiO_2 catalysts [41], Pd/LDH [42]. The results of the above works indicated that the heat treatment of the supports have imposed significant effect on the size and also catalytic activity of the produced catalysts. It has been mentioned that the calcination may influence the catalyst activity via changing the crystalline phase, size of crystallites, and/or surface area of the active phase of the catalyst. Regarding the calcination temperatures used in the present study (<750℃), and also as the calcinations have been performed on the catalysts containing metallic Pd particles, hence, it may only affect the support, rather than the metalic particles doped on the support. As the melting point of the Pd is 1,550℃, which is too far from the used highest calcination temperature (750℃), calcination process cannot change the crystalline phase or size of Pd crystallites. Therfore, the differences observed in the photocatalytic activities of the catalysts by changing of the calcination temperature have been attributed to the effect of calcination on the support particles. The effect of changing calcination temperature on the size or agglomeration of the Pd nanoparticles has been not investigated here, and probably because of the lower Pd content of the catalysts, a pronounced agglomeration of the Pd particles was not observed by increasing of the calcination temperature.

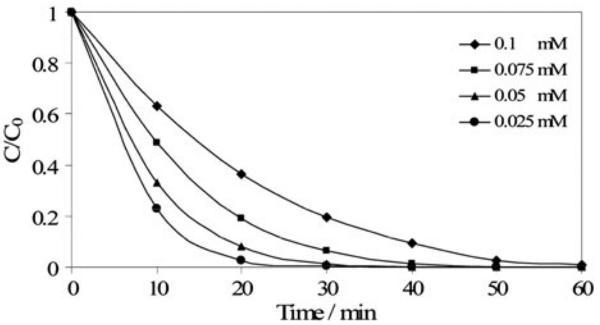

Fig. 8. AY23 concentration ratio as a function of exposure time for different initial AY23 concentrations using 600 mg L^{-1} of 0.75 wt% Pd/TiO_2 photocatalyst calcined at 300˚C.

3.3.2. *Effect of initial AY23 concentration*

The results of the studying of the effect of initial AY23 concentration on the photodegradation efficiency are presented in Fig. 8. It was observed that the photodegradation conversion of AY23 decreases with an increase in the initial concentration of AY23. The presumed reason is that, by increasing of the initial concentration of dye, more and more dye molecules are adsorbed on the surface of TiO_2. This large amount of adsorbed dye is believed to have an inhibitive effect on the reaction of dye molecules with photogenerated holes or hydroxyl radicals, which is due to the lack of any direct contact between them. The increasing of the dye concentration also resulted in the coverage of surface of TiO_2 by the dye molecules, which absorb the light and, consequently, lowers the number of photons reaching to the surface of photocatalyst, thus the photodegradation efficiency decreases [43].

In order to evaluate the degree of mineralization during the photocatalytic treatment, the formation of CO_2 and inorganic ions is generally determined [32], via TOC measurements.

To study the mineralization of AY23 on Pd/TiO_2, dye solution with initial TOC concentration of around 9.6 mg L^{-1} was photodegraded for 120 min at the optimum conditions (600 mg L^{-1} of 0.75 wt% Pd/TiO_2 photocatalyst, calcined at 300˚C, initial AY23 concentration = 0.05 mM; initial solution pH ≈ 6.5; temperature ≈ 25˚C). The measurements of TOC values for the samples taken after 60 and 120 min of UV irradiation of the dye solution revealed that the TOC values were decreased by 50 and 82%, respectively. This indicate that after 120 min of the irradiation, 82% of the initial pollutant dye molecules have been removed from the samples, and the remaining 18% have been converted to small molecules with much more lower environmental toxicities than dye molecules. It is clear that the mineralization does not change in the same way as degree of decolorization and always complete mineralization takes much longer times, which occurs almost by the first degradation reaction of the dye molecule.

For the comparison of the results obtained in this work with the literature, a summary is shown in Table 4. Besides of the extensive literature on the applications of Pd/TiO_2 catalysts, no report has been found dealing with the removal of AY23 by this catalyst. As can be seen in Table 4, relatively promising results have been obtained for the photodegradation of the different organic dyes and chemicals. The highest efficiencies have been observed for the degradation of the pollutants such as Acid Green 16, 90% in 60 min [25], or 73% for formic acid in 30 min [44]. Comparison of the our results with the literature for methyl red and

Table 4
Summary of the literature on the photocatalytic degradation efficiencies of the Pd/TiO_2 photocataysts and the optimum catalyst prepared in this work

Catalyst	Pollutant	Efficiency–time	Reference
Pd–TiO_2,—visible light	Rhodamine B	97%—6.5 h	[46]
Au–Pd–TiO_2 nanotube film	Malathion	172% to TiO_2	[47]
Pd–TiO_2 thin film–UV	Methylene Blue	90%—6 h	[27]
Pd–TiO_2 nanotubes—solar light	Methyl Orange	~100%—2.5–4.5 h	[45]
Pt–Pd-doped TiO_2	Trichloroethylene	35%—30 min	[48]
Pd–TiO_2 film—UV	Formic acid	73%—30 min	[44]
Pd–TiO_2	Phenol	90%	[5]
ZnO–SnO_2—UV	Acid Yellow 23	Decolorization-50 min	[16]
Pd–TiO_2—UV	Acid Green 16	90%—60 min	[25]
Pd–N-doped TiO_2	Natural organic matter	96%	[9]
Pd–TiO_2	NO (gas)	72%	[43]
Pd–TiO_2—UV	Acid Yellow 23	98.6%—30 min	0.75% Pd/TiO_2

methyl orange as dyes with very similar structures to AY23, indicates that the prepared photocatalysts in this work presented much more better results. Mohapatra et al. [45] have prepared the TiO_2 nanotube arrays by the sonoelectrochemical anodization technique and doped with 10 nm Pd nanoparticles. They have found that the prepared Pd doped TiO_2 nanotube arrays can completely photodegrade methyl red and methyl orange dyes under ilumination of simulated solar light for 2.5–4.5 h, meanwhile the 0.75%Pd/TiO_2 photocatalyst could degrade up to 98% of the AY23 dye only in 30 min of irradiation with UV light (Table 4, last row). The improvements observed in the photocatalytic efficincies of the prepared photocatalysts compared to the literature may be attributed to the uniform and efficient dispersion of the monodisperse Pd nanoparticles formed by the microemulsion method. However, more research is required to make exact conclusions on the issue.

4. Conclusion

The AY23 dye was successfully photodegraded using Pd-doped TiO_2 nanoparticles under UV light illumination, and also the effects of different parameters on the photocatalytic efficiencies were investigated. The Pd/TiO_2 nanoparticles were synthesized via two microemulsion method, using *n*-heptane/AOT/water/$NaBH_4$ or $PdCl_2$. The characterization of prepared Pd/TiO_2 photocatalysts using XRD, SEM, EDX, and TEM techniques revealed the presence of uniformly distributed palladium nanoparticles on the surface of TiO_2. According to the TEM micrographs, the distribution of Pd nanoparticles on TiO_2 obtained by microemulsion method was almost uniform with size of around 5–15 nm. It was found that the 0.75 wt% Pd loading has been the optimum loading to achieve the highest efficiency of the AY23 photodegradation. Also, the results showed that the maximum degradation rate (or the optimum conditions to obtain the highest photocatalytic activity) of 0.05 mM AY23 solutions at room temperature has been observed for the experiments carried out using 600 mg L^{-1} of 0.75 wt% Pd/TiO_2 photocatalyst calcined at the optimum temperature of 300˚C and natural pH of reaction medium (pH = 6.5). For the photodegradation reactions carried out at optimum conditions, about 82% reduction in TOC values has been observed after 120 min of reaction time.

Acknowledgment

The authors would like to thank the support of Iranian Nanotechnology Society, University of Tabriz and the Islamic Azad University—Tabriz branch.

References

[1] F. Han, V.S.R. Kambala, M. Srinivasan, D. Rajarathnam, R. Naidu, Tailored titanium dioxide photocatalysts for the degradation of organic dyes in wastewater treatment: A review, Appl. Catal., A 359 (2009) 25–40.

[2] B. Zhu, K. Li, J. Zhou, S. Wang, S. Zhang, S. Wu, W. Huang, The preparation of palladium-modified TiO_2 nanofibers and their photocatalytic performance, Catal. Commun. 9 (2008) 2323–2326.

[3] U.I. Gaya, A.H. Abdullah, Heterogeneous photocatalytic degradation of organic contaminants over titanium dioxide: A review of fundamentals, progress and problems, J. Photochem. Photobiol., C 9 (2008) 1–12.

[4] Z. Wu, Z. Sheng, Y. Liu, H. Wang, N. Tang, J. Wang, Characterization and activity of Pd-modified TiO_2 catalysts for photocatalytic oxidation of NO in gas phase, J. Hazard. Mater. 164 (2009) 542–548.

[5] R. Su, R. Tiruvalam, Q. He, N. Dimitratos, L. Kesavan, C. Hammond, J.A. Lopez-Sanchez, R. Bechstein, C.J. Kiely, G.J. Hutchings, F. Besenbacher, Promotion of phenol photodecomposition over TiO_2 Using Au, Pd, and Au–Pd nanoparticles, ACS Nano 6 (2012) 6284–6292.

[6] V. Tiwari, J. Jiang, V. Sethi, P. Biswas, One-step synthesis of noble metal–titanium dioxide nanocomposites in a flame aerosol reactor, Appl. Catal., A 345 (2008) 241–246.

[7] W.-C. Hung, Y.-C. Chen, H. Chu, T.-H. Ko, Study on photocatalytic degradation of gaseous 1,2-dichloroethane using Pd/TiO_2 and V/TiO_2 prepared by a sol-gel method, Proc. Annu. Conf. Can. Soc. Civ. Eng. 2 (2007) 960–969.

[8] L.R. Quisenberry, L.H. Loetscher, J.E. Boyd, Catalytic inactivation of bacteria using Pd-modified titania, Catal. Commun. 10 (2009) 1417–1422.

[9] T.I. Nkambule, A.T. Kuvarega, R.W.M. Krause, J. Haarhoff, B.B. Mamba, Synthesis and characterisation of Pd-modified N-doped TiO_2 for photocatalytic degradation of natural organic matter (NOM) fractions, Environ. Sci. Pollut. Res. 19 (2012) 4120–4132.

[10] N. Daneshvar, A.R. Khataee, A.R. Ghadim, Decolorization of C.I. Acid Yellow 23 solution by electrocoagulation process: Investigation of operational parameters and evaluation of specific electrical energy consumption (SEEC), J. Hazard. Mater. 148 (2007) 566–572.

[11] T. Tanaka, O. Takahashi, S. Oishi, A. Ogata, Effects of tartrazine on exploratory behavior in a three-generation toxicity study in mice, Reprod. Toxicol. 26 (2008) 156–163.

[12] P.-P. Champagne, J.A. Ramsay, Dye decolorization and detoxification by laccase immobilized on porous glass beads, Bioresour. Technol. 101 (2010) 2230–2235.

[13] S. Pura, G. Atun, Adsorptive removal of acid blue 113 and tartrazine by fly ash from single and binary dye solutions, Sep. Sci. Technol. 44 (2009) 75–101.

[14] N. Modirshahla, M.A. Behnajady, F. Ghanbary, Decolorization and mineralization of C.I. Acid Yellow 23 by Fenton and photo-Fenton processes, Dyes Pigm. 73 (2007) 305–310.

[15] A. Zuorro, R. Lavecchia, Evaluation of UV/H_2O_2 advanced oxidation process (AOP) for the degradation of diazo dye Reactive Green 19 in aqueous solution, Desalin. Water Treat. 52 (2014) 1571–1577.

[16] N. Modirshahla, A. Hassani, M.A. Behnajady, R. Rahbarfam, Effect of operational parameters on decolorization of Acid Yellow 23 from wastewater by UV irradiation using ZnO and ZnO/SnO_2 photocatalysts, Desalination 271 (2011) 187–192.

[17] M. Wawrzkiewicz, Z. Hubicki, Removal of tartrazine from aqueous solutions by strongly basic polystyrene anion exchange resins, J. Hazard. Mater. 164 (2009) 502–509.

[18] M.A. Behnajady, N. Modirshahla, R. Hamzavi, Kinetic study on photocatalytic degradation of C.I. Acid Yellow 23 by ZnO photocatalyst, J. Hazard. Mater. 133 (2006) 226–232.

[19] M.A. Behnajady, N. Modirshahla, N. Daneshvar, M. Rabbani, Photocatalytic degradation of an azo dye in a tubular continuous-flow photoreactor with immobilized TiO_2 on glass plates, Chem. Eng. J. 127 (2007) 167–176.

[20] W. Pang, N. Gao, H. Wang, Sh Xia, A new microfiltration photocatalytic reactor for DDT removal, Desalin. Water Treat. 21 (2010) 303–307.

[21] M.G. Hosseini, M. Shokri, M. Khosravi, R. Najjar, M. Darbandi, Photodegradation of an azo dye by silver-doped nano-particulate titanium dioxide, Toxicol. Environ. Chem. 93 (2011) 1591–1601.

[22] M. Shokri, M.G. Hosseini, M. Khosravi, R. Najjar, Sh Sheikhy, The preparation of Pt-modified TiO_2 nanoparticles via microemulsions, and their application in photocatalytic removal of an azo dye (C.I, Acid Red 27), Fresenius Environ. Bull. 20 (2011) 1063–1068.

[23] A. Mittal, V.K. Gupta, Adsorptive removal and recovery of the azo dye Eriochrome Black T, Toxicol. Environ. Chem. 92 (2010) 1813–1823.

[24] V. Iliev, D. Tomova, L. Bilyarska, L. Petrov, Photooxidation of xylenol orange in the presence of palladium-modified TiO_2 catalysts, Catal. Commun. 5 (2004) 759–763.

[25] S. Sakthivel, M.V. Shankar, M. Palanichamy, B. Arabindoo, D.W. Bahnemann, V. Murugesan, Enhancement of photocatalytic activity by metal deposition: Characterisation and photonic efficiency of Pt, Au and Pd deposited on TiO_2 catalyst, Water Res. 38 (2004) 3001–3008.

[26] N.S. Babu, N. Lingaiah, N. Pasha, J.V. Kumar, P.S.S. Prasad, Influence of particle size and nature of Pd species on the hydrodechlorination of chloroaromatics: Studies on Pd/TiO_2 catalysts in chlorobenzene conversion, Catal. Today 141 (2009) 120–124.

[27] C.-C. Chan, C.-C. Chang, W.-C. Hsu, S.-K. Wang, J. Lin, Photocatalytic activities of Pd-loaded mesoporous TiO_2 thin films, Chem. Eng. J. 152 (2009) 492–497.

[28] V. Uskoković, M. Drofenik, Synthesis of materials within reverse micelles, Surf. Rev. Lett. 12 (2005) 239–277.

[29] M. Boutonnet, S. Lögdberg, E.E. Svensson, Recent developments in the application of nanoparticles prepared from w/o microemulsions in heterogeneous catalysis, Curr. Opin. Colloid Interface Sci. 13 (2008) 270–286.

[30] R. Najjar, C. Stubenrauch, Phase diagrams of microemulsions containing reducing agents and metal salts as bases for the synthesis of metallic nanoparticles, J. Colloid Interface Sci. 331 (2009) 214–220.

[31] R. Najjar, Microemulsions – An Introduction to Properties and Applications, 1st ed., InTech Publisher, Rijeka, Croatia, 2012.

[32] I.K. Konstantinou, T.A. Albanis, TiO_2-assisted photocatalytic degradation of azo dyes in aqueous solution: Kinetic and mechanistic investigations, Appl. Catal., B 49 (2004) 1–14.

[33] K. Vinodgopal, D.E. Wynkoop, P.V. Kamat, Environmental photochemistry on semiconductor surfaces: Photosensitized degradation of a textile azo dye, Acid Orange 7, on TiO_2 particles using visible light, Environ. Sci. Technol. 30 (1996) 1660–1666.

[34] N. Sobana, M. Muruganadham, M. Swaminathan, Nano-Ag particles doped TiO_2 for efficient photodegradation of Direct azo dyes, J. Mol. Catal. A: Chem. 258 (2006) 124–132.

[35] M.R. Hoffmann, S.T. Martin, W. Choi, D.W. Bahnemann, Environmental applications of semiconductor photocatalysis, Chem. Rev. 95 (1995) 69–96.

[36] U.G. Akpan, B.H. Hameed, Parameters affecting the photocatalytic degradation of dyes using TiO_2-based photocatalysts: A review, J. Hazard. Mater. 170 (2009) 520–529.

[37] U.G. Akpan, B.H. Hameed, Photocatalytic degradation of wastewater containing acid red 1 dye by titanium dioxide: Effect of calcination temperature, Desalin. Water Treat. 43 (2012) 84–90.

[38] M. Huang, C. Xu, Z. Wu, Y. Huang, J. Lin, J. Wu, Photocatalytic discolorization of methyl orange solution by Pt modified TiO_2 loaded on natural zeolite, Dyes Pigm. 77 (2008) 327–334.

[39] J. Edwards, J. Pritchard, M. Piccinini, G. Shaw, Q. He, A.F. Carley, ChJ Kiely, G.J. Hutchings, The effect of heat treatment on the performance and structure of carbon-supported Au–Pd catalysts for the direct synthesis of hydrogen peroxide, J. Catal. 292 (2012) 227–238.

[40] J.C. Rooke, T. Barakat, S. Siffert, B.-L. Su, Total catalytic oxidation of toluene using Pd impregnated on hierarchically porous Nb_2O_5 and Ta_2O_5 supports, Catal. Today 192 (2012) 183–188.

[41] I. Yuranov, P. Moeckli, E. Suvorova, Ph. Buffat, L. Kiwi-Minsker, A. Renken, Pd/SiO_2 catalysts: Synthesis of Pd nanoparticles with the controlled size in mesoporous silicas, J. Mol. Catal. A: Chem., 192 (2003) 239–251.

[42] T. Chen, F. Zhang, Y. Zhu, Pd Nanoparticles on layered double hydroxide as efficient catalysts for solvent-free oxidation of benzyl alcohol using molecular oxygen: Effect of support basic properties, Catal. Lett. 143 (2013) 206–218.

[43] C.-H. Wu, Comparison of azo dye degradation efficiency using UV/single semiconductor and UV/coupled semiconductor systems, Chemosphere 57 (2004) 601–608.

[44] B. Xie, Y. Xiong, R. Chen, J. Chen, P. Cai, Catalytic activities of Pd–TiO film towards the oxidation of formic acid, Catal. Commun. 6 (2005) 699–704.

[45] S.K. Mohapatra, N. Kondamudi, S. Banerjee, M. Misra, Functionalization of self-organized TiO_2 nanotubes with Pd nanoparticles for photocatalytic decomposition of dyes under solar light illumination, Langmuir 24 (2008) 11276–11281.

[46] M.M. Mahlambi, A.K. Mishra, S.B. Mishra, A.M. Raichur, B.B. Mambaand R.W. Krause, Layer-by-layer self-assembled metal-ion- (Ag-, Co-, Ni-, and Pd-) doped TiO_2 nanoparticles: Synthesis, characterisation, and visible light degradation of rhodamine B, J. Nanomater. (2012) Article No. 302046.

[47] H. Yu, X. Wang, H. Sun, M. Huo, Photocatalytic degradation of malathion in aqueous solution using an Au–Pd–TiO_2 nanotube film, J. Hazard. Mater. 184 (2010) 753–758.

[48] H.-H. Ou, S.-L. Lo, Effect of Pt/Pd-doped TiO_2 on the photocatalytic degradation of trichloroethylene, J. Mol. Catal. A: Chem. 275 (2007) 200–205.